Cytotherapy 25 (2023) 1293–1299

Contents lists available at ScienceDirect

CYTOTHERAPY

journal homepage: www.isct-cytotherapy.org

Short Report

Three-dimensional cell culture of chimeric antigen receptor T cells originated from peripheral blood mononuclear cells towards cellular therapies

Eduardo Pérez del Río[1,2], Macarena Román Alonso[3,4], Irene Rius[3,4], Fabião Santos[1,2], Miquel Castellote-Borrell[1,5], Jaume Veciana[1,2], Imma Ratera[1,2], Joaquín Arribas[3,4,6,7,**], Judith Guasch[1,2,5,*]

[1] *Institute of Materials Science of Barcelona (ICMAB-CSIC), Bellaterra, Spain*
[2] *Centro de Investigación Biomédica en Red de Bioingeniería, Biomateriales y Nanomedicina (CIBER-BBN), Madrid, Spain*
[3] *Preclinical and Translational Research Program, Vall d'Hebron Institute of Oncology (VHIO), Barcelona, Spain*
[4] *Centro de Investigación Biomédica en Red de Cáncer (CIBERONC), Madrid, Spain*
[5] *Dynamic Biomaterials for Cancer Immunotherapy, Max Planck Partner Group (ICMAB-CSIC), Bellaterra, Spain*
[6] *Institució Catalana de Recerca i Estudis Avançats (ICREA), Barcelona, Spain.*
[7] *Department of Biochemistry and Molecular Biology, Universitat Autònoma de Barcelona, Bellaterra, Spain*

ARTICLE INFO

Article History:
Received 25 November 2022
Accepted 8 August 2023

Key Words:
3D cell culture
3D scaffolds
adoptive cell therapy
CAR T cells
cell expansion
peripheral blood mononuclear cells

ABSTRACT

Background aims: With the objective of improving the *ex vivo* production of therapeutic chimeric antigen receptor (CAR) T cells, we explored the addition of three-dimensional (3D) polystyrene scaffolds to standard suspension cell cultures.
Methods: We aimed to mimic the structural support given by the lymph nodes during *in vivo* lymphocyte expansion.
Results: We observed an increase in cell proliferation compared with standard suspension systems as well as an enhanced cytotoxicity toward cancer cells. Moreover, we directly obtained the CAR T cells from peripheral blood mononuclear cells, thus minimizing the *ex vivo* manipulation of the therapeutic cells and opening the way to synergies among different cell populations.
Conclusions: We propose the use of commercially available 3D polystyrene systems to improve the current immune cell cultures and resulting cell products for emerging cellular (immuno)therapies.

Introduction

Adoptive cellular therapy (ACT) is a novel approach in cancer therapy whereby (autologous) T cells are usually genetically modified and expanded *in vitro* and subsequently reinfused into the patient to mediate tumor destruction [1]. Nevertheless, the large amounts of therapeutic T cells required are challenging to manufacture, especially in the case of endogenous T-cell therapies and those based on tumor-infiltrating lymphocytes [2]. Peripheral blood mononuclear cells (PBMCs) are easily collected from patients and consist of approximately 80% of T and B cells, 10% natural killer cells and 10% monocytes [3]. Thus, they play an important role in the immune response and are rich in T cells, the most commonly used cell population in ACT.

In the past, various studies featuring the use of CAR T cells obtained directly from PBMCs against relapsed and refractory (r/r) B-cell lymphoma and r/r acute lymphoblastic leukemia showed promising results [4–7]. However, this approach was found to yield the potential risk of epitope masking [8], in other words, the (accidental) presence of tumor B cells in the patient sample used to produce CAR T cells, resulting in epitope (CD19) masking by the CAR construct, and consequently escaping from CAR T cells and producing a relapse. This challenge caused most CAR T manufacturers add a (costly) production step based on T-cell purification before CAR T manufacturing. However, approaches to overcome this issue have already been suggested.

* Correspondence: Judith Guasch, Institute of Materials Science of Barcelona (ICMAB-CSIC), Campus UAB, 08193 Bellaterra, Spain.
** Correspondence: Joaquín Arribas, Vall d'Hebron Institute of Oncology (VHIO), 08035 Barcelona, Spain.
E-mail addresses: jarribas@vhio.net (J. Arribas), jguasch@icmab.es (J. Guasch).

https://doi.org/10.1016/j.jcyt.2023.08.003

For example, Quintarelli *et al.* [9] proposed the use of an anti-CD19 CAR short-linker to prevent epitope masking in r/r acute lymphoblastic leukemia. Another challenge in ACT is tackling solid tumors, due to the influence of the tumor microenvironment and its immunosuppressive factors [10]. Towards improving the current outcomes, Payne *et al.* [11] studied the clinical applicability of tumor-sensitized PBMCs of patients with breast cancer expanded and reprogrammed *ex vivo*. The resulting cell population contained activated CD56+ and CD161+ natural killer T cells as well as an enriched tumor-reactive memory T-cell population, a phenotype that is responsible for long-term remissions. The results of this study suggest a synergy between the different cell types that integrate the PBMC population, which may present an advantage over more homogenous T-cell populations.

To date, efforts have been made to improve the *ex vivo* expansion of mostly purified T-cell subsets using biomaterials and tissue-engineering approaches to reach the desired amounts of persistent therapeutic cells *in vivo* [2]. In this case, adding a three-dimensional (3D) scaffold that can mimic the natural secondary lymphoid tissues has been shown to improve T-cell proliferation compared with the standard suspension expansions, in which only magnetic beads coated with the antibodies anti-CD3 and anti-CD28 are used [12–14]. Commercially available 3D polystyrene scaffolds (3D Biotek, Warren, NJ, USA) are an interesting option to explore the behavior of a complex cell population such as the PBMCs, given their structural and physicochemical simplicity. These scaffolds consist of parallel 300-μm-diameter fibers forming layers that are arranged at 90° and offset to each other. The resulting pore size is 400 μm, providing a 100% connectivity within its structure, which allows effective exchange of nutrients and waste between media and cells [15]. To explore the potential of this system capable of conferring a 3D matrix to cell culture, PBMCs as such and modified to express a CAR were cultured in 3D polystyrene scaffolds (Figure 1). In addition, we added Dynabeads (Thermo Fisher Scientific, Waltham, MA, USA) to the culture to mimic the antigen presenting cells [16], as done in relevant clinical studies [17,18]. Dynabeads are magnetic beads of 4.5 μm in size coated with the antibodies anti-CD3 and anti-CD28. The anti-CD3 interacts with the CD3ε chain of the TCR-CD3 complex, resulting in T cell activation, whereas the anti-CD28 provides costimulation to avoid anergy. Finally, T-cell differentiation was also studied, as it is known that less-differentiated cells within the memory T cell subtypes tend to survive longer and expand more efficiently, resulting in better clinical outcomes [19].

Methods

PBMC purification

PBMCs were isolated from buffy coats obtained from adult donors provided by "Banc de Sang i Teixits" (Barcelona, Spain) after the approval of the research project by the "Ethics Committee on Animal and Human Experimentation" of the Autonomous University of Barcelona (Nr. CEEAH 4951). To summarize, PBMCs were separated by density gradient centrifugation from the peripheral blood using Ficoll-Plus-Paque (#70-1440-02; GE Healthcare, Chicago, IL, USA) or Lymphoprep (#07811; Stemcell Technologies, Vancouver, British Columbia, Canada). The interphase layer was collected and incubated with Red Blood Cell Lysis Buffer (#00-4333-57; eBioscience, San Diego, CA, USA) to eliminate remaining red blood cells and washed twice with phosphate-buffered saline (PBS). Isolated PBMCs were counted and directly used or frozen down in heat-inactivated fetal bovine serum (FBS; #10270106, Gibco, Billings, MT, USA) supplemented with 10% dimethyl sulfoxide (#D2650; Merck, Rahway, NJ, USA).

CAR T-cell preparation from PBMCs

P95HER2 CAR T cells containing a CD8 hinge domain with an intracellular CD28 co-stimulatory domain and a CD3z signaling domain were synthesized and cloned into the pMSGV-1 retroviral vector (Genscript, Rijswijk, Netherlands), based on our previously published protocol [20].

Cell culture and seeding

PBMCs were seeded on 96-well plates with 3D polystyrene scaffolds (#Z724300; Merck) 1 day after purification in Roswell Park Memorial Institute 1640 GlutaMAX medium (#61870044, Gibco-Life Technologies, Waltham, MA, USA) supplemented with 10% of human serum (#H4522; Merck), 10 mmol/L of HEPES (#H0887; Merck) and 30 IU/mL interleukin-2 (#RIL2I; Thermo Fisher Scientific). Cells were seeded with Dynabeads (#11131D; Thermo Fisher Scientific) in a 1:1 ratio, as suggested by the manufacturer. A 15-μL drop of a concentrated cell suspension was seeded on top of the 3D polystyrene

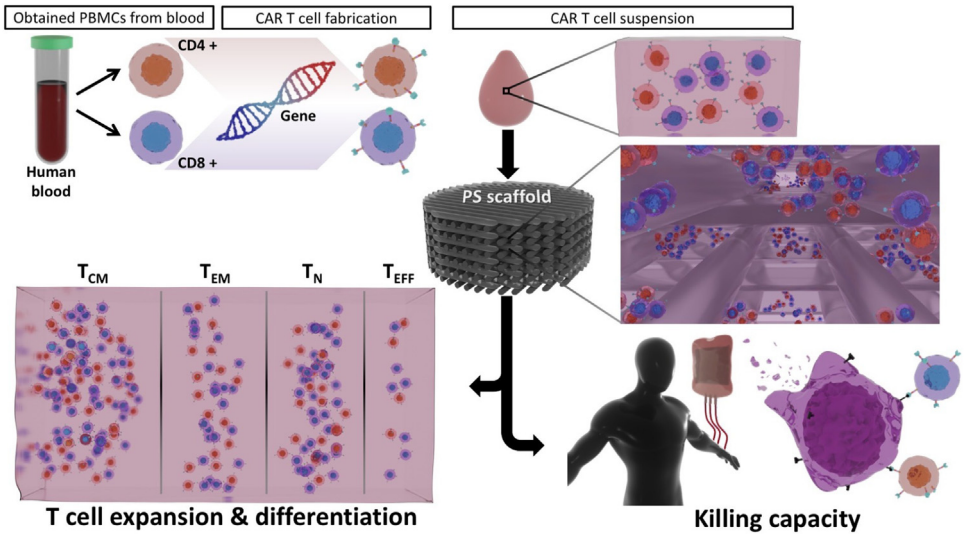

Figure 1. Summary scheme of PMBC cultures, including CAR T-cell formation, in 3D polystyrene scaffolds. (Color version of figure is available online.)

scaffold. After 3 h at 37°C, the medium was added to reach a concentration of 10^6 cells/mL. Positive controls consisted of PBMCs seeded in suspension, i.e., without the 3D scaffold. Negative controls also corresponded to suspension cultures, but did not include Dynabeads. The total volume of each culture well at the day of seeding was 100 μL. At 2 days after seeding, 100 μL of cell media were added to each well.

CAR T cells were seeded on 24-well plates in suspension or in 3D polystyrene scaffolds (#Z687553; Merck) 3 days after transduction in PBMC medium supplemented with 300 IU/mL interleukin-2. Cells were seeded at a concentration of 0.5×10^6 cells/mL. In this case, the total volume of each well was 1 mL at the day of seeding, and 1 extra ml of cell media was added on day 2.

Differentiation and exhaustion assays

PBMC cultures were tested 5 days after seeding. Cell suspensions were prepared in appropriate buffer (PBS and 0.1% FBS) and stained with antihuman CD62L PE (#304840; BioLegend, San Diego, CA, USA), antihuman CD45RO FITC (#21336453; Immunotools GmbH, Friesoythe, Germany) and the corresponding negative controls (PE mouse IgG1, #400112; BioLegend and mouse control IgG2a FITC, #21275523, Immunotools GmbH; respectively) for 30 min at 0°C. Afterwards, they were washed and analyzed by flow cytometry with a BD FACS Canto (BD Biosciences, Franklin Lakes, NJ, USA).

The characterization of expanded CAR T cells was performed after 7 days of culture in suspension or in 3D polystyrene scaffolds by flow cytometry including markers of activation (CD25), exhaustion (Tim3, Lag3, PD-1) and differentiation (CCR7 and CD45RO). For each panel, 0.2×10^6 CAR T cells were isolated, washed twice with PBS and resuspended in a specific buffer (1× PBS, 2.5 mmol/L ethylenediaminetetraacetic acid, 1% bovine serum albumin and 5% horse serum) for 30 min at 4°C. For the exhaustion and activation panels, cells were then labeled with hCD4 BV-421 (#317434; BioLegend), hCD8 APC-Cy7 (#344714; BioLegend), hLag3 PE (#12-2239-42; Invitrogen, Waltham, MA, USA), hPD1 BV605 (#564104; BD Biosciences), hTim3 FITC (#345022; BioLegend) and hCD25 APC (#302610; BioLegend). All antibodies were used at 1/300 dilution except for hCD8 APC-Cy7, used at 1/500. Fluorescence minus one controls were included to define the negative gates for selected populations. For the differentiation panel, cells were stained with 1/300 hCD4 BV 421 (#317434; BioLegend), 1/500 hCD8 APC-Cy7 (#344714; BioLegend), 1/100 hCCR7 BV650 (#353234; BioLegend) and 1/1000 hCD45RO PE (#304205; BioLegend). In addition, CAR expression was assessed by labeling cells with 1/20 biotinylated mIgG (#115-065-072, Jackson ImmunoResearch, West Grove, PA, USA) and streptavidin APC (#405207k; BioLegend) at 1/150. Zombie Aqua (#423101; BioLegend) at 1/1000 dilution was used as a viability marker. Data was acquired on a FACS Celesta (BD Biosciences).

Proliferation assays

Nonenriched PBMCs were stained before seeding with a carboxyfluoroscein succinimidyl ester (CFSE) cell proliferation kit (#C34554; Life Technologies). In summary, 1 μL of CFSE stock solution (5 mmol/L) was diluted in 99 μL of PBS with a 5% FBS. Cells were diluted in PBS up to a final volume of 900 μL and put in contact with 100 μL of the diluted CFSE solution through rapid agitation and incubated for 5 min at room temperature in the dark. After the incubation, 10 mL of ice-cold PBS with 5% FBS was added to quench the staining. Then, cells were centrifuged and resuspended in media (Roswell Park Memorial Institute and 10% FBS) to achieve a concentration of 10^6 stained cells/mL. At 5 days after seeding, cells were analyzed by flow cytometry with a BD FACS Canto (BD Biosciences).

Due to the greater time of study of the proliferation of CARs, including re-seedings and changes of media, and limitations of the CFSE cell proliferation technique, the number of resulting CARs for each check point (days 4th and 9th) was obtained by collecting all the cells for each condition and counting them three times with a Neubauer chamber. For the growth rate, the number of accumulated cells was calculated for an initial number of 1.5×10^6 cells.

CAR T cytotoxicity assay

Target epithelial cells positive and negative for the target antigen were harvested with trypsin–ethylenediaminetetraacetic acid (#11560626; Gibco), stained with 1/500 cell tracer CFSE (#C34554; Invitrogen) and seeded in 96-well plates at 10^4 cells/well in PBMC media. 24 h later, CAR T cells were added at several target/CAR T ratios. After 48 h of the co-coculture, cells were harvested, washed with PBS and stained with Zombie Aqua (1/1000) as a viability cell marker. Viable CFSE-positive cells were counted using an LSR Fortessa or a FACS Canto (BD Biosciences).

Software

The flow cytometry data were analyzed using the software FlowJo (FlowJo LLC) and the graphs were performed in Origin (OriginLab Corporation, Northampton, MA, USA) or Microsoft Excel (Microsoft, Redmond, WA, USA). In the box plots, the boxes correspond to the interquartile ranges defined by the 25th and 75th percentiles, the central line is the median, the whiskers show 1 standard deviation, × defines 1st and 99th percentiles, – represents the maximum and minimum and the square (□) is the average. Statistical tests were performed in Origin.

Results

Primary human PBMC proliferation was assessed through the expansion, replication and proliferation indexes [21] after staining cells with CFSE. CFSE is an intracellular dye that is only fluorescent in viable cells and whose intensity is sequentially halved upon cell division, therefore allowing to precisely study cell proliferation [22]. The expansion and replication indexes are defined by the fold-expansion of the whole population and of responding cells, respectively. A greater value in these parameters correlates with a larger quantity of cells after cell culture, being the expansion index the most important one for ACT, as it gives the final number of cells available for therapy. The replication and proliferation indexes, the latter being the number of divisions that cells from the original population have undergone divided by the number of divided cells, only consider the number of responsive cells, i.e., cells that have been triggered by the proliferative stimulus. These indexes have been chosen in this first proof-of-concept step, as they provide more information about the characteristics of the proliferative process than the final numbers relevant for the clinics. After 5 days of culture, the proliferation of PBMCs seeded in 3D polystyrene scaffolds was evaluated, resulting in an increase in all the three parameters (Figure 2A).

After normalizing the data to the positive control, i.e., the state-of-the-art expansion system, which consists of cells expanded in suspension using Dynabeads, we obtained an expansion index of 1.68, i.e., an improvement of a 68% was achieved when using 3D polystyrene scaffolds. The replication and proliferation indexes showed median values of 1.52 and 1.17, respectively. These results are in agreement with a previous study employing primary human CD4+ T cells seeded on 3D polystyrene scaffolds [14]. In fact, PBMCs show greater proliferation rates in comparison with the CD4+ T-cell experiments, possibly due to the presence and synergy between the different types of cell populations that compose the PBMCs [23]. As previously mentioned, not only 3D polystyrene scaffolds present an excellent connectivity with open size pores that allow the adequate diffusion of cells and nutrients but also

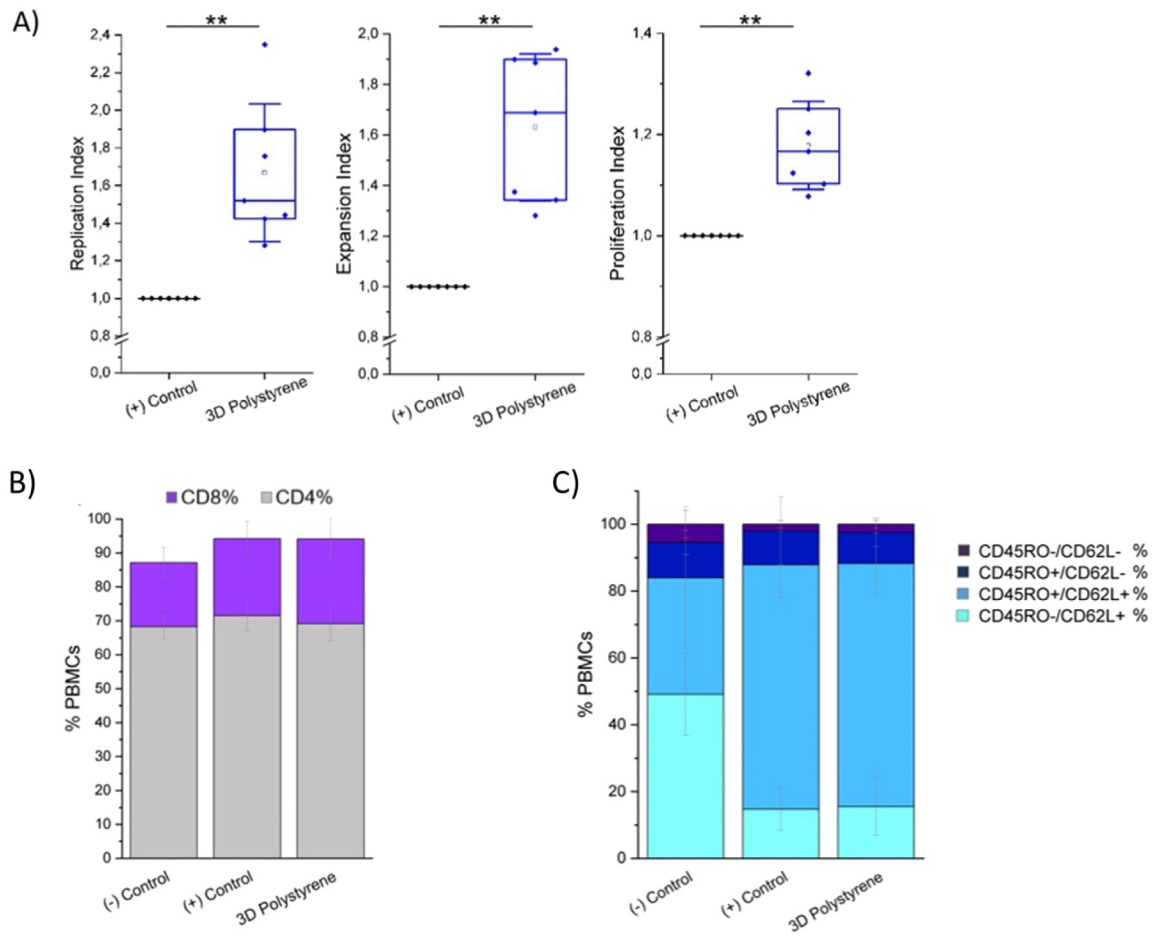

Figure 2. (A) Normalized proliferation analysis of primary human PBMCs 5 days after activation with Dynabeads and seeding in suspension (positive control) and in 3D polystyrene scaffolds (Ndonors = 7). (B) Percentage of CD3+CD4+ and CD3+CD8+ T-cell subsets within PBMCs. The bar chart summarizes the percentage of CD4+ (gray) and CD8+ (purple) T cells within PBMCs (Ndonors = 6) cultured in suspension with (positive control) and without (negative control) Dynabeads, as well as cells expanded with Dynabeads in a 3D polystyrene scaffold. (C) Differentiation analysis of PBMCs 5 days after seeding (Ndonors = 6). Statistical significance was determined by the Mann–Whitney *U* test in all cases (**P* < 0.05, ***P* < 0.01). (Color version of figure is available online.)

present a mechanically strong structure [15], which may assist lymphocyte cell migration [24] and enhance the contact with Dynabeads. According to these results, we conclude that the structure of these 3D polystyrene scaffolds is beneficial for PBMC overall proliferation, which could possibly be further improved, for example, by adding chemical stimuli.

After demonstrating that the 3D polystyrene scaffolds increased PBMC proliferation, the CD4/CD8 ratio after expansion was analyzed (Figure 2B). The median percentage of CD4+ T cells in the negative control was of 67.3%, whereas in the positive control increased to 72.8%. The value obtained with the 3D polystyrene scaffold was of 69.0%. These results show that after activation, the percentage of CD3+CD4+ T cells seems to be greater, especially on the positive control. Similarly, the median percentage of the CD3+CD8+ cells in the negative control was of 18.9%, which increased after activation to 21.5% in the positive control and 25.0% for T cells seeded in the 3D polystyrene scaffold. The scaffold may therefore have a slight tendency to favor the CD3+CD8+ proportion 5 days after T-cell activation compared with the expansion in suspension. A greater proportion of CD8+ T cells would be interesting, as they are the major subset or subset of choice in ACT, due to their effector cytotoxic function and enhanced antitumor activity [25]. However, the differences observed in our system were not found significant, and in general terms, the higher percentage of CD4+ versus CD8+ T cells in the PBMCs agrees with the reported 2:1 ratio found in peripheral blood [26].

In addition, the differentiation degree of cultured cells was analyzed through the CD45RO/CD62L surface markers (Figures 2C and supplementary Figure 1). CD45RO is a surface protein expressed by human leukocytes and used as a marker of memory T cells [27]. CD62L, also named L-selectin, is a type I transmembrane cell adhesion molecule expressed on most circulating leukocytes [28]. These markers allow to differentiate between naïve and stem cell memory (CD45RO−/CD62L+), central memory (CD45RO+/CD62L+), effector memory (CD45RO+/CD62L−) and effector (CD45RO-/CD62L−) T cells [29]. The resulting phenotypes analyzed with this procedure hardly changed for cells activated in suspension or in the 3D polystyrene scaffolds. The percentage of CD45RO−/CD62L+ cells decreased from a mean value of 49.1% for the inactivated cells (or negative control) to 14.7% for cells activated in suspension (or positive control) and 15.5% for cells seeded and activated in 3D polystyrene scaffolds. These values resulted in a significant decrease of this phenotype for activated cells, but no significant differences were observed due to the effect of the 3D system. Similarly, CD45RO+/CD62L+ cells increased from a mean percentage of 34.9% in the negative control, to a mean value of 73.3% in the positive control and 72.8% for the 3D polystyrene scaffold, showing significant differences only due to cell activation. No significant change was observed for CD45RO+/CD62L− cells, i.e., similar values of 10.6%, 10.1% and 9.3% were obtained for the negative and positive controls and 3D polystyrene, respectively. Finally, the results of the CD45RO-/CD62L- population were below 10% for all conditions. In conclusion, the results show that 3D polystyrene scaffolds can

enhance PBMC proliferation compared to cultures in suspension, without affecting their CD4/CD8 ratio or phenotype.

In the next step, we studied the culture of CAR T cells (Figure 3), which were obtained from PBMCs. In particular, we used the recently described p95HER2 CAR T cells [20]. The tumor-specific antigen p95HER2 is a truncated form of the tyrosine kinase receptor HER2 [30], which is especially amplified in breast and some gastrointestinal tumors [31].

For proliferation studies, we analyzed the cultures on days 4 and 9, and performed reseedings to keep cell concentrations below $2–3 \times 10^6$ cells/mL. After 4 days of expansion, the resulting median number of cells achieved with the standard expansion method (suspension system) was of 5.9×10^6 cells, whereas CAR T cells produced from PBMCs seeded in the 3D polystyrene scaffold achieved a median value of 6.8×10^6 cells (Figure 3A), i.e., a 15% increase, as shown with the normalized data to the positive control (Figure 3B), which helps minimize donor-to-donor variability. At day 9, the increasing tendency was maintained, being 19.3×10^6 the median number of cells obtained with the suspension system and 24.7×10^6 the median number of CAR T cells produced with the 3D polystyrene scaffold

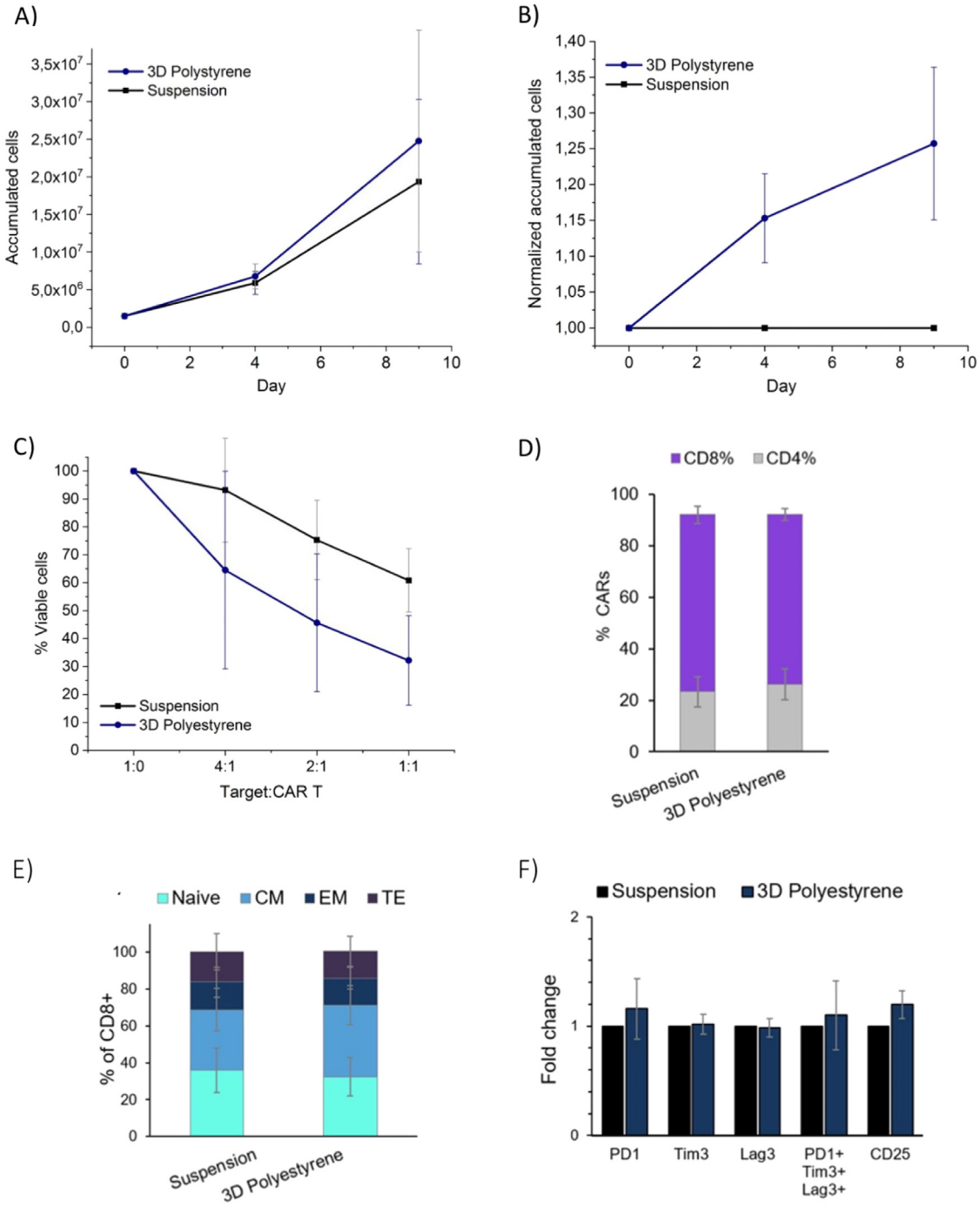

Figure 3. (A) Number of accumulated CAR T cells produced from PBMCs seeded in suspension and in 3D polystyrene scaffolds (Ndonors = 3). (B) Number of accumulated CAR T cells produced from PBMCs normalized to the cells obtained in suspension. (C) Cytotoxicity assay of CAR T cells expanded in suspension or in 3D polystyrene scaffolds using co-cultures with antigen-positive cells at different target/CAR T cells ratios (Ndonors = 2). (D) Percentage of CD4+ and CD8+ cells among the alive cells analyzed by flow cytometry (Ndonors = 3). (E) Differentiation analysis of the resulting CAR+CD8+ T cells produced from PBMCs at day 10 (Ndonors = 3). (F) Analysis of exhaustion and activation markers on CAR+CD8+ T cells normalized to % of positive cells for each marker in the suspension condition (Ndonors = 3). (Color version of figure is available online.)

(Figure 3A). Thus, a 25% increase in the number of cells was achieved with the 3D platform, showing its beneficial effect on the expansion of these cells (Figure 3B).

Once it was proven that the 3D scaffold could increase the number of expanded CAR T cells, we performed a complete characterization of the resulting cells, analyzing their killing capacity and phenotype at day 10 post-transduction. Thus, we determined the effect of the 3D polystyrene scaffold on the quality and functionality of CAR T cells. For assessing the killing capacity and specificity, we co-cultured the expanded CAR T cells with target cells expressing or not the p95HER2 antigen [20], at different effector to target ratios (Figure 3C). The results were normalized so that the 100% of target cell viability was determined by the number of viable target cells remaining after co-culture with the lowest ratio of CAR T cells expanded in a conventional suspension culture. When CAR T cells were co-cultured with antigen-positive cells, a significant increase in the killing capacity of the 3D polystyrene-expanded CAR T cells was observed at the lowest target cell/CAR T cell ratio (4:1), compared with CAR T cells expanded in the absence of the scaffold. Specifically, the percentage of alive target cells was of 93.2% in comparison with the median value of 64.5% for those cells seeded in the 3D polystyrene scaffold. Increasing the ratio to 2:1, the percentages of viable cancer cells decreased to median values of 75.3% in the case of CAR T cells seeded in suspension and 45.7% for CAR T cells seeded in 3D scaffolds. Finally, using a 1:1 ratio, a median percentage of 60.8% of viable cancer cells was achieved for the suspension condition and of 32.2% for the 3D polystyrene scaffolds. In addition, the same assay was performed on cells not expressing the CAR-targeted antigen and no significant differences in cell killing were observed in any of the conditions, suggesting that the 3D polystyrene-expanded CAR T cells increased their cytotoxic effect while retained their specificity towards the cognate antigen. These results show that using the 3D scaffold for the expansion of CAR T cells produced from PBMCs not only increases the number of resulting cells, but also their antigen-specific killing capacity. Finally, the phenotype of the expanded CAR T cells was examined. Specifically, the CD4/CD8 ratio, differentiation, exhaustion and activation status at day 10 post-transduction were analyzed in both culturing conditions. Results revealed no significant differences between both expansion conditions in terms of CD4/CD8 ratio, as seen before for the non-transduced PBMC population. In this case, CD8+ cells were found to be the main population, contributing to approximately 70% of the total cell number, whereas the CD4+ fraction remained smaller (approximately 25%) (Figure 3D). For this reason and the fact that CD8+ T cells are the most used in the clinics, the rest of the phenotypic results are shown for CD8+ T cells.

Thus, we analyzed the differentiation degree of CD8+ T cells based on the expression of the CD45RO and CCR7 markers (Figure 3E). CCR7 is a chemokine receptor known to regulate CD8+ T-cell homing to the secondary lymphoid organs, and it is used to evaluate the difference between phenotypes [32]. CD8+ T cells were defined as naïve and stem cell memory (CD45RO−/CCR7+), central memory (CD45RO+/CCR7+), effector memory (CD45RO+/CCR7−) or terminal effector (CD45RO−/CCR7−). CAR T cells showed similar phenotypes independently of the expansion methodology used, i.e., 3D scaffolds or in suspension. Specifically, the majority of the population corresponded to naïve, stem cell memory and central memory cell phenotypes, which are associated with greater anti-tumor activity, and only approximately 15% of CD8+ T cells showed a terminal differentiation phenotype. Similar results were obtained for CD4+ T cells (supplementary Figure 2).

Moreover, CAR T-cell functionality was assessed by flow cytometric detection of upregulated exhaustion and activation markers. In particular, the negative immune checkpoints Tim3, Lag3 and PD1 [33], and the early/middle activation marker CD25 [34] were used (Figure 3F). The percentage of positive cells for each marker in the culture with 3D polystyrene scaffolds was normalized to the percentage of positive cells in the standard suspension system and expressed as fold change. The percentage of cells positive for the three exhaustion markers was also assessed (PD1+Tim3+Lag3+). Results showed no significant differences between both culture systems, although a slight increase in the CD25 activation marker was observed when using the 3D polystyrene scaffold.

All together, these results revealed that, despite the increased proliferation ratio of CAR T cells in the 3D polystyrene scaffolds, no increase in differentiation, exhaustion and activation markers was observed. In other words, culturing CAR T cells in this 3D system yields a larger number of total CAR T cells at the end of the expansion without seeming to increase tonic signaling of the expanded CAR T cell product, which is associated to impaired antitumoral effects [29,35,36].

Conclusions

In conclusion, PBMCs and CAR T cells directly produced from PBMCs were cultured in 3D polystyrene scaffolds in order to resemble the 3D matrix of the lymph nodes, and study its influence on cell expansion, phenotype and functionality. It was shown that the use of 3D polystyrene scaffolds increased PBMC proliferation, achieving significantly higher values for the expansion, proliferation and replication indexes, possibly due to enhanced cell–cell interactions through confinement. Also, the resulting CD8/CD4 ratios and phenotypes obtained were analyzed, showing no significant differences. Similarly, the 3D polystyrene scaffolds increased the expansion of the clinically desired CAR T cells and their killing capacity, without affecting the phenotype, exhaustion and activation markers of the resulting cells. Thus, the 3D polystyrene scaffolds are an interesting option for human PBMC culture, either as such or transduced to result in CAR T-cell production. It is also worth mentioning that in this last case, the cell product fabrication process would benefit from reduced *ex vivo* manipulation of the therapeutic cells compared to more purified T cell populations. Additionally, synergies could occur among different cell populations [11], which could especially be useful in solid tumors such as the HER2+ here used as proof-of-concept, to help counteracting the tumor microenvironment. However, potential issues such as epitope masking should be taken into account. In addition, the 3D polystyrene scaffolds could be coated with cytokines and cell adhesive molecules, such as CCL21 and ICAM-1 [37,38], to introduce chemical stimuli to further enhance CAR T cell proliferation and/or functionality. The use of 3D polystyrene scaffolds opens a way to more effective and economic cultures to be used in the emerging ACT or laboratory models compared to standard suspension systems. Moreover, they could be incorporated to bioreactors by adapting their design and subsequent lithography fabrication process.

Author Contributions

Conception and design of the study: JA and JG. Acquisition of data: EPdR, MRA, I Rius, FS and MCB. Analysis and interpretation of data: EPdR, MRA and I Rius. Drafting or revising the manuscript: EPdR, MRA, MCB, JV, I Ratera, JA and JG. All authors have approved the final article.

Declaration of Competing Interest

The authors have no commercial, proprietary or financial interest in the products or companies described in this article.

Funding

This research was funded by Instituto de Salud Carlos III through Consorcio Centro de Investigación Biomédica en Red (CIBER) with the projects “Alycia” (Nr. BBN18PI01) and “Gels4ACT” (Nr. BBN20PIV02). The authors are also grateful for the financial support received from the Spanish Ministry of Science and Innovation (PID2020-115296RA-

I00, PID2019-105622RBI00 and the "Ramón y Cajal" program [RYC-2017-22614]). The work was supported as well by the Max Planck Society through the Max Planck Partner Group "Dynamic Biomimetics for Cancer Immunotherapy" in collaboration with the Max Planck for Medical Research (Heidelberg, Germany). This research was also supported by the European Union's Horizon 2020 research and innovation programme H2020-MSCA-COFUND-2016 (DOC-FAM, grant agreement Nr. 754397). The authors acknowledge financial support from the Spanish Ministry of Science and Innovation through the "Severo Ochoa" Programme for Centres of Excellence in R&D (CEX2019-000917-S).

Acknowledgments

We acknowledge D. P. Rosenblatt for proofreading the manuscript, X. Rodriguez Rodriguez for assisting us in the blood transportation, C. Bernadó for assistance in the project management and funding acquisition and E. Arenas for fruitful discussions. This work has been developed inside the "Materials Science" PhD program of UAB.

Supplementary materials

Supplementary material associated with this article can be found in the online version at doi:10.1016/j.jcyt.2023.08.003.

References

[1] Barbari C, Fontaine T, Parajuli P, Lamichhane N, Jakubski S, Lamichhane P, Deshmukh RR. Immunotherapies and combination strategies for immuno-oncology. Int. J. Mol. Sci. 2020;21:5009.
[2] Isser A, Livingston NK, Schneck JP. Biomaterials to enhance antigen-specific T cell expansion for cancer immunotherapy. Biomaterials 2021;268:120584.
[3] Acosta Davila JA, Hernandez De Los Rios A. An overview of peripheral blood mononuclear cells as a model for immunological research of *Toxoplasma gondii* and other apicomplexan parasites. Front. Cell. Infect. Microbiol. 2019;9:24.
[4] Neelapu SS, Locke FL, Bartlett NL, Lekakis LJ, Miklos DB, Jacobson CA, Braunschweig I, Oluwole OO, Siddiqi T, Lin Y, Timmerman JM, Stiff PJ, Friedberg JW, Flinn IW, Goy A, Hill BT, Smith MR, Deol A, Farooq U, McSweeney P, Munoz J, Avivi I, Castro JE, Westin JR, Chavez JC, Ghobadi A, Komanduri KV, Levy R, Jacobsen ED, Witzig TE, Reagan P, Bot A, Rossi J, Navale L, Jiang Y, Aycock J, Elias M, Chang D, Wiezorek J, Go WY. Axicabtagene ciloleucel CAR T-cell therapy in refractory large B-cell lymphoma. N. Eng. J. Med. 2017;377:2531–44.
[5] Locke FL, Ghobadi A, Jacobson CA, Miklos DB, Lekakis LJ, Oluwole OO, Lin Y, Braunschweig I, Hill BT, Timmerman JM, Deol A, Reagan PM, Stiff P, Flinn IW, Farooq U, Goy A, McSweeney PA, Munoz J, Siddiqi T, Chavez JC, Herrera AF, Bartlett NL, Wiezorek JS, Navale L, Xue A, Jiang Y, Bot A, Rossi JM, Kim JJ, Go WY, Neelapu SS. Long-term safety and activity of axicabtagene ciloleucel in refractory large B-cell lymphoma (ZUMA-1): A single-arm, multicentre, phase 1–2 trial. Lancet Oncol 2019;20:31–42.
[6] Davila ML, Riviere I, Wang X, Bartido S, Park J, Curran K, Chung SS, Stefanski J, Borquez-Ojeda O, Olszewska M, Qu J, Wasielewska T, He Q, Fink M, Shinglot H, Youssif M, Satter M, Wang Y, Hosey J, Quintanilla H, Halton E, Bernal Y, Bouhassira DCG, Arcila ME, Gonen M, Roboz GJ, Maslak P, Douer D, Frattini MG, Giralt S, Sadelain M, Brentjens R. Efficacy and toxicity management of 19-28z CAR T cell therapy in B cell acute lymphoblastic leukemia. Sci. Transl. Med. 2014;6:224ra25.
[7] Brentjens RJ, Davila ML, Riviere I, Park J, Wang X, Cowell LG, Bartido S, Stefanski J, Taylor C, Olszewska M, Borquez-Ojeda O, Qu J, Wasielewska T, He Q, Bernal Y, Rijo IV, Hedvat C, Kobos R, Curran K, Steinherz P, Jurcic J, Rosenblat T, Maslak P, Frattini M, Sadelain M. CD19- targeted T cells rapidly induce molecular remissions in adults with chemotherapy-refractory acute lymphoblastic leukemia. Sci. Transl. Med. 2013;5:177ra38.
[8] Lemoine J, Ruella M, Houot R. Born to survive: How cancer cells resist CAR T cell therapy. J. Hematol. Oncol. 2021;14:1–12.
[9] Quintarelli C, Guercio M, Manni S, Boffa I, Sinibaldi M, Cecca SD, Caruso S, Abbaszadeh Z, Camera A, Cembrola B, Ciccone R, Orfao A, Martin-Martin L, Gutierrez-Herrero S, Herrero-Garcia M, Cazzaniga G, Nunes V, Songia S, Marcatili P, Marin FI, Ruella M, Bertaina V, Vinti L, Bufalo FD, Algeri M, Merli P, Angelis BD, Locatelli F. Strategy to prevent epitope masking in CAR.CD19+ B-cell leukemia blasts. J. Immunother. Cancer 2021;9:e001514.
[10] Srivastava S, Riddell SR. Chimeric antigen receptor T cell therapy: Challenges to bench-to-bedside efficacy. J. Immunol. 2018;200:459–68.
[11] Payne KK, Zoon CK, Wan W, Marlar K, Keim RC, Kenari MN, Kazim AL, Bear HD, Manjili MH. Peripheral blood mononuclear cells of patients with breast cancer can be reprogrammed to enhance anti-HER-2/neu reactivity and overcome myeloid-derived suppressor cells. Breast Cancer Res. Treat. 2013;142:45–57.
[12] Santos F, Valderas-Gutiérrez J, Pérez del Río E, Castellote-Borrell M, Rodriguez XR, Veciana J, Ratera I, Guasch J. Enhanced human T cell expansion with inverse opal hydrogels. Biomater. Sci. 2022;10:3730–8.
[13] Pérez del Río E, Santos F, Rodriguez XR, Martínez- Miguel M, Roca-Pinilla R, Arís A, Garcia-Fruitós E, Veciana J, Spatz JP, Ratera I, Guasch J. CCL21-loaded 3D hydrogels for T cell expansion and differentiation. Biomaterials 2020;259:120313.
[14] Pérez del Río E, Martinez Miguel M, Veciana J, Ratera I, Guasch J. Artificial 3D culture systems for T cell expansion. ACS Omega 2018;3:5273–80.
[15] Caicedo-Carvajal CE, Liu Q, Remache Y, Goy A, Suh KS. Cancer tissue engineering: A novel 3D polystyrene scaffold for in vitro isolation and amplification of lymphoma cancer cells from heterogeneous cell mixtures. J. Tissue Eng. 2011;2011:1–10.
[16] Trickett A, Kwan YL. T cell stimulation and expansion using anti-CD3/CD28 beads. J. Immunol. Methods 2003;275:251–5.
[17] Frey NV, Gill S, Hexner EO, Schuster S, Nasta S, Loren A, Svoboda J, Stadtmauer E, Landsburg DJ, Mato A, Levine BL, Lacey SF, Melenhorst JJ, Veloso E, Gaymon A, Pequignot E, Shan X, Hwang W-T, June CH, Porter DL. Long-term outcomes from a randomized dose optimization study of chimeric antigen receptor modified T cells in relapsed chronic lymphocytic leukemia. J. Clin. Oncol. 2020;38:2862–71.
[18] Turtle CJ, Hay KA, Hanafi L-A, Li D, Cherian S, Chen X, Wood B, Lozanski A, Byrd JC, Heimfeld S, Riddell SR, Maloney DG. Durable molecular remissions in chronic lymphocytic leukemia treated with CD19-specific chimeric antigen receptor–modified T cells after failure of ibrutinib. J. Clin. Oncol. 2017;35:3010–20.
[19] Tantalo DG, Oliver AJ, Scheidt Bv, Harrison AJ, Mueller SN, Kershaw MH, Slaney CY. Understanding T cell phenotype for the design of effective chimeric antigen receptor T cell therapies. J. Immunother. Cancer 2021;9:e002555.
[20] Román, M.; Rius-Ruiz, I.; Grinyó-Escuer, A.; Duro-Sánchez, S.; Escorihuela, M.; Moessner, E.; Klein, C.; Arribas, J. Humanized CAR T cells targeting p95HER2. *bioRxiv* 2022. 2022.05.20.492812.
[21] Roederer M. Interpretation of cellular proliferation data: Avoid the panglossian. Cytom. A 2011;79A:95–101.
[22] Lyons AB, Parish CR. Determination of lymphocyte division by flow cytometry. J. Immunol. Methods 1994;171:131–7.
[23] Blasco E, Barra A, Nicolas M, Lecron JC, Wijdenes J, Preud'homme JL. Proliferative response of human CD4+ T lymphocytes stimulated by the lectin jacalin. Eur. J. Immunol. 1995;25:2010–8.
[24] Saitakis M, Dogniaux S, Goudot C, Bufi N, Asnacios S, Maurin M, Randriamampita C, Asnacios A, Hivroz C. Different TCR-induced T lymphocyte responses are potentiated by stiffness with variable sensitivity. eLife 2017;6:e23190.
[25] Jackson SR, Yuan J, Teague RM. Targeting CD8+ T- cell tolerance for cancer immunotherapy. Immunotherapy 2014;6:833–52.
[26] Lozano-Ojalvo D, López-Fandiño R, López-Expósito I. PBMC-derived T cells. In: Verhoeckx K, Cotter P, López- Expósito I, Kleiveland C, Lea T, Mackie A, eds. The impact of food bioactives on health: In vitro and ex vivo models, Cham (Switzerland): Springer; 2015:169–80.
[27] Valentine M, Song K, Maresh GA, Mack H, Huaman MC, Polacino P, Ho O, Cristillo A, Kyung Chung H, Hu S-L, Pincus SH. Expression of the memory marker CD45RO on helper T cells in macaques. PLOS One 2013;8:e73969.
[28] Ivetic A. A head-to-tail view of l-selectin and its impact on neutrophil behaviour. Cell Tissue Res 2018;371:437–53.
[29] Sommermeyer D, Hudecek M, Kosasih PL, Gogishvili T, Maloney DG, Turtle CJ, Riddell SR. Chimeric antigen receptor-modified T cells derived from defined CD8+ and CD4+ subsets confer superior antitumor reactivity in vivo. Leukemia 2016;30:492–500.
[30] Arribas J, Baselga J, Pedersen K, Parra-Palau JL. p95HER2 and breast cancer. Cancer Res 2011;71:1515–9.
[31] Arenas EJ, Martínez-Sabadell A, Rius Ruiz I, Román Alonso M, Escorihuela M, Luque A, Fajardo CA, Gros A, Klein C, Arribas J. Acquired cancer cell resistance to T cell bispecific antibodies and CAR T targeting HER2 through JAK2 down-modulation. Nat. Commun. 2021;12:1237.
[32] Samji T, Khanna KM. Understanding memory CD8+ T cells. Immunol. Lett. 2017;185:32–9.
[33] Datar I, Sanmamed MF, Wang J, Henick BS, Choi J, Badri T, Dong W, Mani N, Toki M, Mejías LD, Lozano MD, Perez-Gracia JL, Velcheti V, Hellmann MD, Gainor JF, McEachern K, Jenkins D, Syrigos K, Politi K, Gettinger S, Rimm DL, Herbst RS, Melero I, Chen L, Schalper KA. Expression analysis and significance of PD-1, LAG-3, and TIM- 3 in human non–small cell lung cancer using spatially resolved and multiparametric single-cell analysis. Clin. Cancer Res. 2019;25:4663–73.
[34] Caruso A, Licenziati S, Corulli M, Canaris AD, De Francesco MA, Fiorentini S, Peroni L, Fallacara F, Dima F, Balsari A, Turano A. Flow cytometric analysis of activation markers on stimulated T cells and their correlation with cell proliferation. Cytometry 1997;27:71–6.
[35] Gattinoni L, Lugli E, Ji Y, Pos Z, Paulos CM, Quigley MF, Almeida JR, Gostick E, Yu Z, Carpenito C, Wang E, Douek DC, Price DA, June CH, Marincola FM, Roederer M, Restifo NP. A human memory T cell subset with stem cell-like properties. Nat. Med. 2011;17:1290–7.
[36] Eyquem J, Mansilla-Soto J, Giavridis T, van der Stegen SJC, Hamieh M, Cunanan KM, Odak A, Gönen M, Sadelain M. Targeting a CAR to the TRAC locus with CRISPR/CAS9 enhances tumour rejection. Nature 2017;543:113–7.
[37] Adutler-Lieber S, Friedman N, Geiger B. Expansion and antitumor cytotoxicity of T-cells are augmented by substrate-bound CCL21 and intercellular adhesion molecule 1. Front. Immunol. 2018;9:1303.
[38] Adutler-Lieber S, Zaretsky I, Sabany H, Kartvelishvily E, Golani O, Geiger B, Friedman N. Substrate-bound CCL21 and ICAM1 combined with soluble IL-6 collectively augment the expansion of antigen-specific murine CD4(+) T cells. Blood Adv 2017;1:1016–30.